EuroIntervention
2025;21:e217-e228
published online e-edition February 2025
DOI: 10.4244/EIJ-D-24-00720

ORIGINAL RESEARCH

Functional or anatomical assessment of non-culprit lesions in acute myocardial infarction

Xueming Xu[1-3], MD; Chao Fang[1-3], MD, PhD; Senqing Jiang[1-3], MD, PhD; Yuzhu Chen[1-3], MD; Jiawei Zhao[1-3], MD; Sibo Sun[1-3], MD; Yini Wang[1-3], MD, PhD; Lulu Li[1-3], MS; Dongxu Huang[1-3], MD; Shuang Li[1-3], MD; Huai Yu[1-3], MD, PhD; Tao Chen[1-3], MD, PhD; Jinfeng Tan[1-3], MD; Xiaohui Liu[1-3], MD, PhD; Jiannan Dai[1-3], MD, PhD; Gary S. Mintz[4], MD; Bo Yu[1-3]*, MD, PhD

X. Xu and C. Fang contributed equally as first authors.
**Corresponding author: Department of Cardiology, The 2nd Affiliated Hospital of Harbin Medical University, 246 Xuefu Road, Nangang District, Harbin, 150086, China. E-mail: yubodr@163.com*

This paper also includes supplementary data published online at: https://eurointervention.pcronline.com/doi/10.4244/EIJ-D-24-00720

ABSTRACT

BACKGROUND: Previous studies have reported the value of quantitative flow ratio (QFR) to assess the physiological significance of non-culprit lesions (NCLs) in acute myocardial infarction (AMI) patients and of optical coherence tomography (OCT)-defined thin-cap fibroatheroma (TCFA) to identify non-culprit vulnerable plaques.

AIMS: We sought to systematically compare long-term NCL-related clinical prognosis in an AMI population utilising acute Murray fractal law-based QFR (μQFR) values and OCT-defined TCFA.

METHODS: Three-vessel OCT imaging and μQFR assessment were conducted in 645 AMI patients, identifying 1,320 intermediate NCLs in non-infarct-related arteries. The primary endpoint was a composite of cardiac death, NCL-related non-fatal myocardial infarction (MI), and NCL-related unplanned coronary revascularisation, with follow-up lasting up to 5 years.

RESULTS: The primary endpoint occurred in 59 patients (11.1%). OCT-defined TCFA independently predicted patient-level (adjusted hazard ratio [HR] 3.05, 95% confidence interval [CI]: 1.80-5.19) and NCL-specific primary endpoints (adjusted HR 4.46, 95% CI: 2.33-8.56). The highest event rate of 29.6% was observed in patients with NCLs that were TCFA (+) with μQFR ≤0.80, compared to 16.3% in those that were also TCFA (+) but with μQFR >0.80, 6.0% in those that were TCFA (–) with μQFR ≤0.80, and 6.6% in those that were TCFA (–) with μQFR >0.80 (log-rank p<0.001). TCFA was an independent predictor for the primary endpoint in ST-segment elevation MI (STEMI; adjusted HR 3.27, 95% CI: 1.67-6.41) and non-STEMI (adjusted HR 3.26, 95% CI: 1.24-8.54) patients, whereas μQFR ≤0.80 was not.

CONCLUSIONS: When assessing NCLs during the index procedure in AMI patients, OCT-defined TCFA serves as the dominant prognostic predictor for long-term clinical outcomes, rather than μQFR-determined physiological significance.

KEYWORDS: acute myocardial infarction; Murray fractal law-based quantitative flow ratio; optical coherence tomography; prognostic implication

SUBMITTED ON 07/08/2024 - REVISION RECEIVED ON 1st 16/10/2024 / 2nd 20/11/2024 - ACCEPTED ON 21/11/2024

Non-culprit lesions (NCLs) in patients with acute myocardial infarction (AMI) may be associated with an increased risk of future adverse cardiac events[1-3]. In addition to coronary angiography, coronary physiology and plaque morphology are two ways to evaluate these lesions[4].

Although invasive physiological assessment for intermediate coronary stenosis is the standard care in stable patients, its superiority for achieving complete revascularisation in AMI patients remains controversial. Previous studies have suggested that fractional flow reserve (FFR) may underestimate lesion severity during the acute phase, while the instantaneous wave-free ratio (iFR) might overestimate it[5,6], raising concerns about their reliability for evaluating NCLs, especially at the time of primary percutaneous coronary intervention (PCI)[7,8]. So far, head-to-head comparisons between FFR-guided and conventional angiography-guided strategies for evaluating NCLs have produced inconsistent results[9,10], and a recent study indicated that FFR-guided complete revascularisation during the index hospitalisation did not yield better outcomes compared to a culprit-only strategy[11]. Quantitative flow ratio (QFR), enabling estimation of FFR from coronary angiography[12-15], may be superior to guidewire-based coronary physiology when assessing NCLs in an AMI population[16-18]. Murray fractal law-based QFR (μQFR), the latest generation of QFR, enables rapid FFR calculation from a single angiographic view, with high diagnostic accuracy for functionally significant coronary stenosis[19].

Intravascular optical coherence tomography (OCT)-defined thin-cap fibroatheroma (TCFA) has been shown to be efficacious when assessing intermediate NCLs in stable as well as AMI patients, including those who were FFR-negative[20-22].

This study aimed to systematically investigate the association of acute μQFR values and OCT-defined TCFA with long-term NCL-related clinical prognosis during the index procedure of patients presenting with an AMI at both the patient and lesion levels.

Editorial, see page e198

Impact on daily practice

The present large-scale observational analysis suggests that optical coherence tomography (OCT)-defined thin-cap fibroatheroma (TCFA) is significantly predictive of both patient-level and lesion-specific non-culprit lesion (NCL)-related clinical outcomes, irrespective of Murray fractal law-based quantitative flow ratio (μQFR) values and acute myocardial infarction (AMI) presentation at admission, whereas the prognostic implication of a μQFR ≤0.80 was insignificant in this analysis. These insights provide robust evidence that OCT-identified NCL TCFA during the index procedure for AMI has greater clinical relevance than μQFR-determined coronary physiology for long-term clinical outcomes, emphasising the critical value of OCT in assessing NCL in patients with AMI.

Methods

STUDY POPULATION

Patients qualified for inclusion if they were aged 18 years or older, had successfully undergone primary or urgent PCI of the culprit lesion for AMI (ST-segment elevation myocardial infarction [STEMI] or non-STEMI [NSTEMI]), and had undergone OCT examination of all three major epicardial coronary arteries. The main exclusion criteria were cardiogenic shock, end-stage renal disease, severe liver dysfunction, and contrast allergy. Patients with left main disease, chronic total occlusion, extreme tortuosity, or severe calcification were also excluded because of potential difficulties in performing OCT. This was a retrospective study of 1,118 eligible AMI patients who underwent three-vessel OCT imaging at the Second Affiliated Hospital of Harbin Medical University (Harbin, China) between January 2017 and May 2019. Among them, 235 patients were excluded from the analysis for the following reasons: (i) suboptimal OCT imaging (i.e., massive thrombus) or short OCT pullback less than two-thirds of the artery length (n=164); (ii) previous PCI or coronary artery bypass grafting (n=62); (iii) coronary spasm due to the OCT procedure (n=2); and (iv) in-hospital death (n=7). We further excluded 151 patients without intermediate NCLs on coronary angiography (i.e., 30-90% visible diameter stenosis), 61 patients exhibiting NCLs solely in infarct-related arteries (IRAs), 20 patients with poor angiographic quality, and 6 patients with severe vessel overlap or tortuosity. Ultimately, 645 patients with evaluable three-vessel OCT imaging and μQFR data were included in the study and received scheduled clinical follow-up after discharge **(Figure 1)**.

The study was approved by the ethics committee of our institution, and all patients provided written informed consent. The diagnostic criteria for AMI, means of identification of the culprit lesion at baseline, and detailed definitions of traditional coronary risk factors are presented in **Supplementary Appendix 1**.

ANGIOGRAPHY ACQUISITION AND ANALYSIS

Coronary angiography was performed using standard techniques. Quantitative coronary angiographic analyses were performed for eligible NCLs (i.e., 30-90% visible diameter stenosis) using the Cardiovascular Angiography Analysis System (CAAS) version 5.10.1 (Pie Medical Imaging). After selection of end-diastolic frames and calibration using the catheter tip, the reference vessel diameter, minimal lumen diameter, diameter stenosis, and lesion length were measured.

μQFR COMPUTATION AND ANALYSIS

Offline μQFR analysis of NCLs in non-IRAs was conducted using AngioPlus Core 2.0 (Pulse Medical Technology), based

Abbreviations

μQFR	Murray fractal law-based quantitative flow ratio	**IRA**	infarct-related artery	**PCI**	percutaneous coronary intervention
AMI	acute myocardial infarction	**NCL**	non-culprit lesion	**TCFA**	thin-cap fibroatheroma
		OCT	optical coherence tomography		

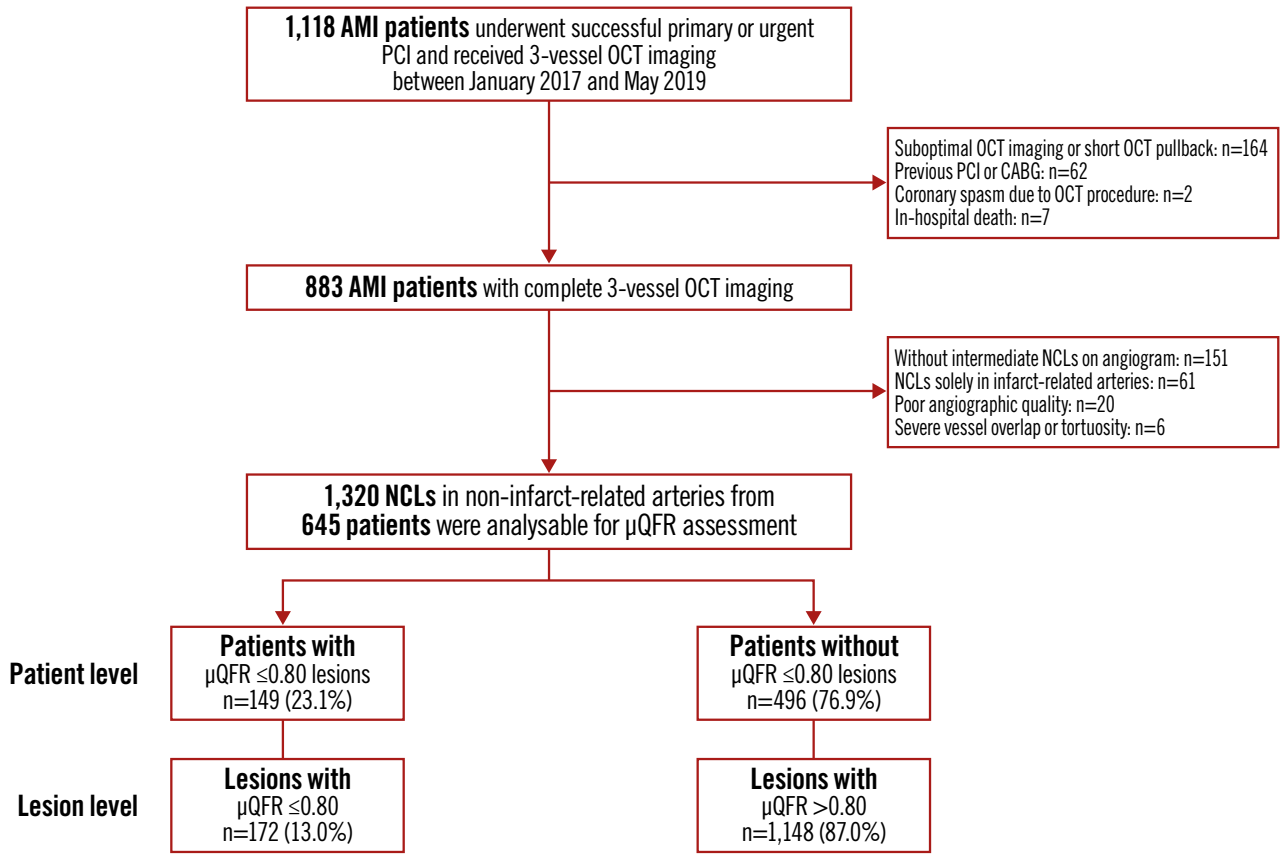

Figure 1. *Study flowchart. In this study, the full analysis set included 645 AMI patients, encompassing a total of 1,320 NCLs. Among these, 149 patients (23.1%) were identified, with 172 NCLs between them (13.0%) having a μQFR ≤0.80, and the remaining 496 patients (76.9%) presented with NCLs all exhibiting a μQFR >0.80. μQFR: Murray fractal law-based quantitative flow ratio; AMI: acute myocardial infarction; CABG: coronary artery bypass grafting; NCL: non-culprit lesion; OCT: optical coherence tomography; PCI: percutaneous coronary intervention*

on angiograms from the index procedure, by investigators blinded to OCT data and clinical outcomes. In this study, a new generation of artificial intelligence (AI)-powered μQFR was used for calculation[19]. The detailed methodology for μQFR computation has been reported previously[19] and is described in **Supplementary Appendix 1**. Briefly, from a single angiographic projection with optimal visualisation (minimal foreshortening and vessel overlap), hyperaemic flow velocity was calculated by dividing the length of the centreline by the contrast dye filling time of the artery. A key frame with a sharp luminal contour on a major epicardial coronary artery containing the evaluable NCL was selected for subsequent analysis. Luminal contours of scanned vessels and major side branches were automatically delineated and manually corrected as needed. AI algorithms based on Murray's fractal law were used to reconstruct the reference diameter function. Finally, pressure drop was calculated using fluid dynamic equations with hyperaemic flow velocity as a boundary condition, and μQFR was available for each NCL. In this study, we analysed 1,320 intermediate NCLs from 952 vessels in 645 patients with AMI, demonstrating an average of 1.39 NCLs per vessel, which is a relatively reasonable number. However, there is currently no clear consensus on how to address the effects of tandem lesions on μQFR measurements. To minimise the impact of tandem lesions on μQFR calculations, our study estimated μQFR for each individual lesion. We referenced the work by Guan et al[23], which utilised the "virtual stent technique", a built-in function of the μQFR system. In this method, a "virtually implanted stent" is marked using stent length markers at the precise location of the implantation site, with proximal and distal markers specified to obtain ΔμQFR. The system then calculates the μQFR of the target NCL as 1.0 minus ΔμQFR. An NCL was considered flow-limiting if the μQFR was ≤0.80, a threshold that has been widely utilised in recent studies[15,17-19,24]. Patients with at least one NCL with μQFR ≤0.80 are termed the μQFR-positive group, while patients with exclusively μQFR >0.80 lesions are termed the μQFR-negative group.

OCT IMAGING ACQUISITION AND ANALYSIS

OCT imaging was acquired using a commercially available frequency domain system (OPTIS [Abbott]), first, in the treated infarct-related artery and, then, in the non-infarct-related arteries. All OCT images were analysed in the Intravascular Imaging and Physiology Core Lab of our centre by analysts who were blinded to patient outcomes. Coregistration of the angiograms and OCT was performed automatically or using

fiduciary points (i.e., side branches) when online angiographic coregistration was not successful.

The OCT analyses have been detailed in **Supplementary Appendix 1**[25,26]. Briefly, NCLs identified by OCT were untreated coronary segments with luminal narrowing and a loss of the normal vessel wall architecture (i.e., intima, media, and adventitia)[27]. After successful intervention of the culprit lesion, NCLs that were deemed to be clearly severe (i.e., >90% angiographic diameter stenosis) and/or had a Thrombolysis in Myocardial Infarction flow <3 were also eligible for revascularisation. Management was left to the discretion of the interventional cardiologist, and lesions scheduled for staged revascularisation were also excluded from the study. To be considered as two separate NCLs in the same vessel, the intervening reference segment had to be at least 5 mm in length on the longitudinal OCT view. TCFA was defined as lipidic plaque with the thinnest fibrous cap thickness <65 µm and a maximum lipid arc >180°[20-22].

CLINICAL FOLLOW-UP

Follow-up information was obtained at 1, 3, 6, and 12 months after discharge and annually thereafter by clinical visit or telephone contact. Patients were censored at 5 years (with a 30-day window) or at the last known contact. For the patient-level analysis, the primary endpoint was a composite of adverse cardiac events, including cardiac death, NCL-related non-fatal myocardial infarction (MI), and NCL-related unplanned coronary revascularisation. For the lesion-level analysis, cardiac death without an angiogram at the time of the event was not included. All clinical outcomes were defined according to the Academic Research Consortium guidelines, and detailed definitions of adverse cardiac events are provided in **Supplementary Appendix 1**[28]. An independent clinical endpoint committee consisting of three experienced interventional cardiologists (T. Chen, J. Tan, and X. Liu), who were blinded to the OCT and µQFR data, reviewed and adjudicated all events. When possible, each new MI or revascularisation was assigned to a specific coronary lesion by comparison of baseline and event angiograms, and an NCL-related event was adjudicated as occurring in initially untreated coronary segments.

STATISTICAL ANALYSIS

Categorical variables have been presented as n (%) and were compared using the Pearson's chi-squared test or the Fisher's exact test, depending on the size of the category cell. Normality of continuous data was assessed using the Kolmogorov-Smirnov test. Continuous variables are presented as mean±standard deviation (SD) or median (interquartile range [IQR]) and were compared using the Student's t-test or the Mann-Whitney U test, respectively. Data were analysed on a per-patient basis for clinical characteristics and on a per-lesion basis for comparison of lesion characteristics and physiological indices. To account for the potential clustering effects of multiple NCLs within a single patient, we used generalised estimating equations to compare characteristics of NCLs with µQFR ≤0.80 and µQFR >0.80. Estimated means±SD are presented as summary statistics. Independent predictors of µQFR ≤0.80 were determined by a binary logistic regression model which included independent variables demonstrating a significant association in the univariate analyses (p<0.05). Prior to this, variance inflation factors (VIF) were calculated through linear regression analysis to assess the presence of multicollinearity among the independent variables, with a VIF value of less than 10 often considered an acceptable threshold, indicating that multicollinearity is not a major concern. The Kaplan-Meier estimator was used to calculate time-to-first event rates, and a log-rank test was performed to assess the differences in event-time distributions among groups. A univariate Cox proportional hazards regression model was used to estimate the hazard ratio (HR) and its corresponding 95% confidence interval (CI). A multivariate Cox proportional hazards regression model was used to identify adjusted prognostic factors. The patient-level multivariate model included clinically relevant baseline variables (age, sex, coronary risk factors, and clinical presentation). The lesion-level multivariate model was adjusted for other OCT characteristics with significant effects on clinical outcomes in the univariable analysis assessed within the same NCL (p<0.05). Statistical analyses were performed using SPSS 26.0 (IBM), with a 2-tailed p-value <0.05 considered statistically significant.

Results

BASELINE CLINICAL CHARACTERISTICS

Baseline clinical characteristics are summarised in **Table 1**. The average age of the 645 patients was 58.1±11.1 years, with 25.7% being female and 69.9% presenting with STEMI. Offline µQFR assessment indicated that 149 (23.1%) patients had at least one NCL with a µQFR ≤0.80, while 496 (76.9%) patients had no NCL with a µQFR ≤0.80. Patients with at least one lesion with a µQFR ≤0.80 were characterised by older age, higher female representation, and STEMI on admission. Medication use at discharge was comparable among groups regardless of µQFR stratification.

DIFFERENT LESION CHARACTERISTICS BETWEEN µQFR ≤0.80 VERSUS µQFR >0.80

A total of 1,320 untreated intermediate NCLs (median 2.0 [IQR 1.0-3.0] per patient) were identified. The mean diameter stenosis of these lesions was 42.4±10.1%, and the mean µQFR was 0.90±0.10 **(Table 2)**. Specifically, µQFR was positive (≤0.80) in 172 lesions (13.0%) and negative (>0.80) in 1,148 lesions (87.0%). Lesions with µQFR ≤0.80 were more frequently located in the left anterior descending artery (LAD), exhibited greater angiographic diameter stenosis, and had a higher prevalence of TCFA (26.2% vs 18.8%; p=0.025) compared to those with µQFR >0.80 **(Table 2)**. Additionally, the presence of cholesterol crystals (32.6% vs 21.8%; p=0.004) and layered tissue (63.4% vs 46.9%; p<0.001) were more common in µQFR-positive lesions.

In the multivariable analysis, only LAD location (odds ratio [OR] 2.23, 95% CI: 1.51-3.27; p<0.001), lipid core length (OR 1.04, 95% CI: 1.02-1.05; p<0.001), and minimal lumen area (OR 0.41, 95% CI: 0.34-0.51; p<0.001) were independently associated with µQFR ≤0.80 **(Supplementary Table 1)**. The VIF calculated using linear regression indicated no evidence of multicollinearity among the independent variables **(Supplementary Table 2)**.

Table 1. Baseline clinical characteristics.

	Overall patients (N=645)	μQFR-positive group (n=149, 23.1%)	μQFR-negative group (n=496, 76.9%)	*p*-value
Age, years	58.1±11.1	59.7±10.4	57.6±11.3	0.043
Female	166 (25.7)	48 (32.2)	118 (23.8)	0.039
Coronary risk factors				
Hypertension	289 (44.8)	72 (48.3)	217 (43.8)	0.325
Dyslipidaemia	379 (58.8)	88 (59.1)	291 (58.7)	0.932
Diabetes mellitus	157 (24.3)	33 (22.1)	124 (25.0)	0.477
Current smoker	326 (50.5)	69 (46.3)	257 (51.8)	0.238
CKD: eGFR <60 mL/min/1.73 m^2	66 (10.2)	20 (13.4)	46 (9.3)	0.143
Clinical presentation				**0.046**
STEMI	451 (69.9)	114 (76.5)	337 (67.9)	
Non-STEMI	194 (30.1)	35 (23.5)	159 (32.1)	
Laboratory data				
Total cholesterol, mg/dL	175.0±51.5	168.4±52.6	177.0±51.1	0.083
Triglycerides, mg/dL	116.1 [79.7-174.5]	123.2 [90.3-169.3]	115.6 [77.3-180.3]	0.289
LDL-C, mg/dL	108.9±40.4	104.0±39.5	110.4±40.6	0.093
HDL-C, mg/dL	48.7±15.9	47.4±14.5	49.0±16.3	0.291
hs-CRP, mg/L	4.5 [2.1-9.3]	4.5 [1.9-10.2]	4.5 [2.1-9.2]	0.759
HbA1c, %	6.2±1.3	6.3±1.3	6.2±1.4	0.763
Medication at discharge				
Aspirin	640 (99.2)	147 (98.7)	493 (99.4)	0.713
$P2Y_{12}$ inhibitor	639 (99.1)	147 (98.7)	492 (99.2)	0.912
Ticagrelor	380 (58.9)	86 (57.7)	294 (59.3)	0.735
Clopidogrel	271 (42.0)	62 (41.6)	209 (42.1)	0.909
Dual antiplatelet therapy	635 (98.4)	146 (98.0)	489 (98.6)	0.602
Statins	641 (99.4)	146 (98.0)	495 (99.8)	0.061

Values are n (%), mean±SD, or median [IQR]. μQFR: Murray fractal law-based quantitative flow ratio; CKD: chronic kidney disease; eGFR: estimated glomerular filtration rate; HbA1c: glycated haemoglobin c; HDL-C: high-density lipoprotein cholesterol; hs-CRP: high-sensitivity C-reactive protein; IQR: interquartile range; LDL-C: low-density lipoprotein cholesterol; SD: standard deviation; STEMI: ST-segment elevation myocardial infarction

CLINICAL OUTCOMES DURING FOLLOW-UP

Patients were followed for up to 5 years (median of 4.1 [IQR 3.7-4.7] years), with 17 patients (2.6%) either lost to follow-up or refusing to provide follow-up information. Among the 645 patients, 76 experienced adverse cardiac events (cumulative rate 13.9%): 22 had culprit lesion-related events (cumulative rate 3.6%), 39 had NCL-related events (cumulative rate 7.6%), and 20 had cardiac deaths without angiograms at the time of events, rendering the responsible lesions indeterminate (cumulative rate 3.7%) **(Figure 2)**.

The primary endpoint occurred in 59 patients (cumulative rate 11.1%), including 20 cardiac deaths, 10 patients with NCL-related non-fatal MIs, and 36 patients with NCL-related unplanned coronary revascularisations **(Supplementary Table 3)**. In the lesion-level analysis, 42 NCLs were identified with event angiography and matching baseline OCT, including 11 lesions with a non-fatal MI and 39 lesions with an unplanned coronary revascularisation. Angiographic diameter stenosis of NCLs leading to events increased significantly from 47.9±10.2% at baseline to 63.4±16.6% at the time of event (p<0.001). The same was true when limited to lesions leading to an unplanned coronary revascularisation (48.3±10.5% at baseline vs 63.9±16.9% at the time of event; p<0.001).

PROGNOSTIC IMPLICATIONS OF μQFR AND OCT-DEFINED TCFA

In **Figure 3**, Kaplan-Meier curves illustrate the composite clinical outcomes categorised by μQFR and TCFA at the patient and lesion levels. The risk of the primary endpoint was consistently higher in patients with at least one NCL with a μQFR ≤0.80 (16.2% vs 9.6%, HR 1.92, 95% CI: 1.13-3.28) **(Figure 3A)** or TCFA (20.5% vs 6.5%, HR 3.28, 95% CI: 1.95-5.51) **(Figure 3B)** compared to their counterparts, with a more pronounced difference in the divergence of the survival curves for patients stratified by TCFA. These properties generally held for the lesion-level analysis (for μQFR ≤0.80: HR 2.77, 95% CI: 1.42-5.41; for TCFA: HR 4.65, 95% CI: 2.54-8.52) **(Figure 3C, Figure 3D)**. Complete patient-level and lesion-level multivariable models are presented in **Supplementary Table 4** and **Supplementary Table 5**. In the multivariate analysis, OCT-defined TCFA (adjusted HR 3.05, 95% CI: 1.80-5.19) was independently associated with the primary endpoint, and the hazard proportionality remained consistent in the

Table 2. Comparative analysis of NCL characteristics between those with μQFR ≤0.80 and μQFR >0.80.

Lesion characteristics	Overall lesions (N=1,320)	Lesions with μQFR ≤0.80 (n=172, 13.0%)	Lesions with μQFR >0.80 (n=1,148, 87.0%)	*p*-value
Coronary physiology index				
μQFR	0.90±0.10	0.68±0.12	0.93±0.04	<0.001
Angiographic characteristics				
Lesion location	<0.001			
LAD	445 (33.7)	92 (53.5)	353 (30.7)	<0.001
LCx	428 (32.4)	53 (30.8)	375 (32.7)	0.574
RCA	447 (33.9)	27 (15.7)	420 (36.6)	<0.001
Reference vessel diameter, mm	3.1±1.4	2.8±0.5	3.1±1.5	0.003
Minimal lumen diameter, mm	1.8±0.8	1.3±0.4	1.8±0.8	<0.001
Diameter stenosis, %	42.4±10.1	54.3±11.4	40.7±8.6	<0.001
Lesion length, mm	17.4±9.1	22.1±11.7	16.7±8.4	<0.001
OCT characteristics				
Distance from coronary ostium to MLA site, mm	32.0±28.7	30.2±16.9	32.3±30.1	0.383
Minimal fibrous cap thickness, μm	105.7±56.2	102.2±58.7	106.3±55.8	0.399
Mean lipid arc, °	170.9±49.6	179.6±52.4	169.4±48.9	0.018
Lipid core length, mm	12.8±10.0	17.0±12.0	12.1±9.5	<0.001
TCFA	261 (19.8)	45 (26.2)	216 (18.8)	0.025
MLA, mm^2	3.3±1.9	1.8±1.1	3.5±1.9	<0.001
Lumen area stenosis, %	59.1±15.0	70.7±14.2	57.4±14.3	<0.001
Other qualitative characteristics				
Non-culprit plaque rupture	100 (7.6)	17 (9.9)	83 (7.2)	0.165
Thrombus	47 (3.6)	7 (4.1)	40 (3.5)	0.675
Calcification	592 (44.8)	85 (49.4)	507 (44.2)	0.162
Macrophage	1,206 (91.4)	164 (95.3)	1,042 (90.8)	0.064
Microchannel	749 (56.7)	93 (54.1)	656 (57.1)	0.529
Cholesterol crystals	306 (23.2)	56 (32.6)	250 (21.8)	0.004
Layered tissue	647 (49.0)	109 (63.4)	538 (46.9)	<0.001

Values are n (%) or mean±SD. μQFR: Murray fractal law-based quantitative flow ratio; LAD: left anterior descending artery; LCx: left circumflex artery; MLA: minimal lumen area; NCL: non-culprit lesion; OCT: optical coherence tomography; RCA: right coronary artery; TCFA: thin-cap fibroatheroma

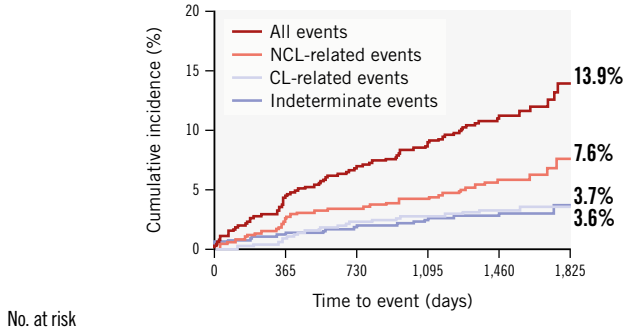

Figure 2. *Longitudinal Kaplan-Meier curves for adverse cardiac events incidence. Among the 645 patients, the Kaplan-Meier curves indicate that the highest cumulative incidence of adverse cardiac events was observed for NCL-related events (7.6%). This was followed by indeterminate events (3.7%) and CL-related events (3.6%). CL: culprit lesion; NCL: non-culprit lesion*

multivariable analysis at the lesion level (adjusted HR 4.46, 95% CI: 2.33-8.56) **(Table 3)**. Conversely, the presence of an NCL with a μQFR ≤0.80 was not significantly associated with the occurrence of the primary endpoint (adjusted HR 1.37, 95% CI: 0.79-2.40).

Patients and lesions were divided into 4 groups based on μQFR values and the presence or absence of TCFA **(Figure 4)**. In the patient-level analysis, the highest event rate of 29.6% was observed in patients with NCLs that were TCFA (+) with μQFR ≤0.80, compared to 16.3% in those that were also TCFA (+) but with μQFR >0.80, 6.0% in those that were TCFA (–) with μQFR ≤0.80, and 6.6% in those that were TCFA (–) with μQFR >0.80 (log-rank p<0.001) **(Figure 4A)**. Similar results were obtained at the lesion level, with event rates of 17.4%, 9.7%, 4.3%, and 2.1%, respectively (log-rank p<0.001) **(Figure 4B)**. The subgroup analysis indicated that the presence of TCFA, regardless of μQFR values, had significant prognostic value for future adverse clinical outcomes **(Supplementary Figure 1, Supplementary Figure 2)**. **Table 4** showed that OCT-defined TCFA was independently associated with the risk of the primary endpoint in both STEMI (adjusted HR 3.27, 95% CI: 1.67-6.41) and NSTEMI patients (adjusted HR 3.26, 95% CI: 1.24-8.54). In contrast, μQFR ≤0.80 did not

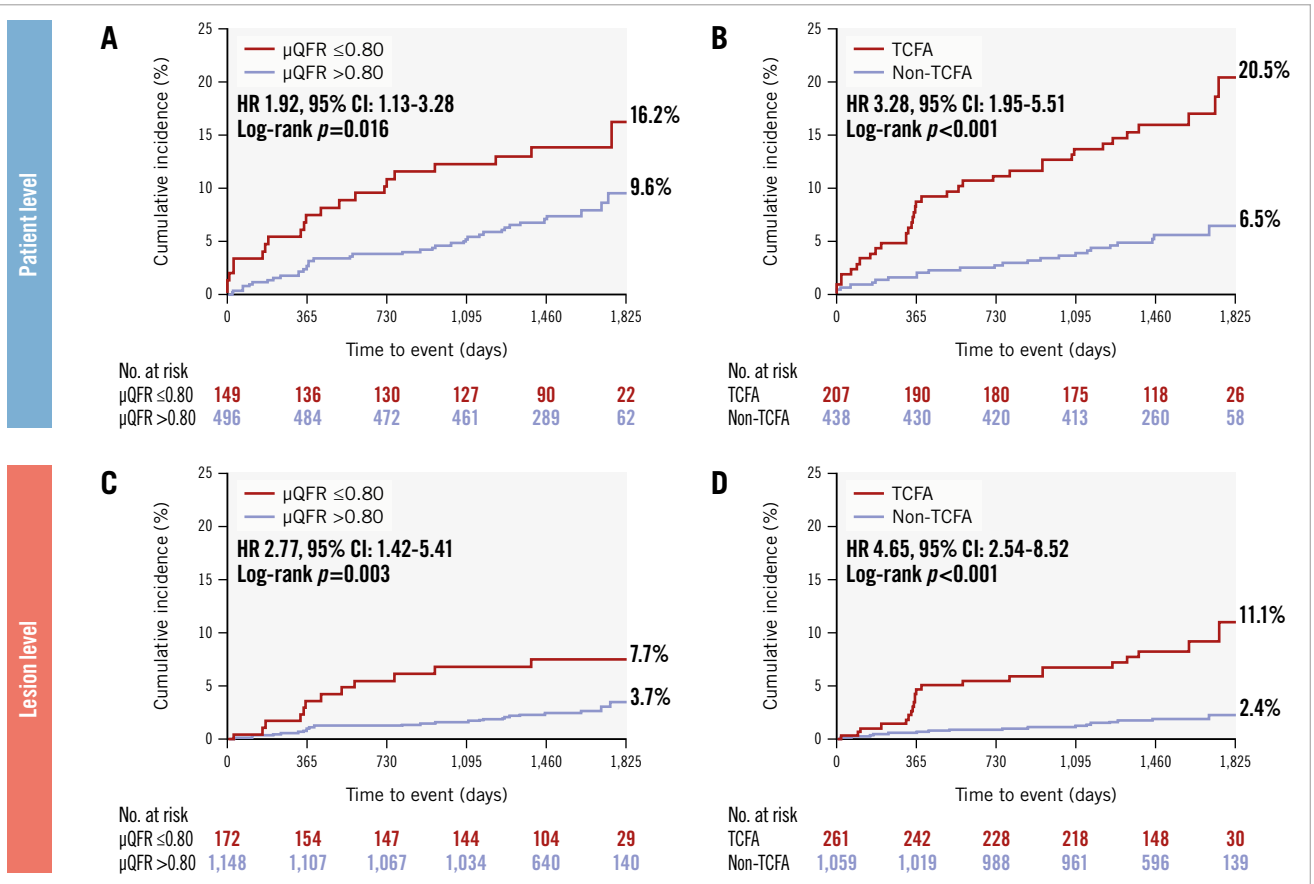

Figure 3. *Individual prognostic value of μQFR and OCT-defined TCFA in patient-level and lesion-level analyses. The risk of NCL-related clinical events was significantly higher in patients with (A) μQFR ≤0.80 or (B) TCFA, compared to their counterparts. These properties generally held at the lesion level for NCLs with (C) μQFR ≤0.80 or (D) TCFA. μQFR: Murray fractal law-based quantitative flow ratio; CI: confidence interval; HR: hazard ratio; OCT: optical coherence tomography; TCFA: thin-cap fibroatheroma*

Table 3. Multivariable analysis for NCL-related clinical events at the patient and lesion levels.

	Adjusted HR (95% CI)	*p*-value
Patient-level model[a]		
μQFR (≤0.80 vs >0.80)	1.37 (0.79-2.40)	0.266
TCFA	3.05 (1.80-5.19)	<0.001
Lesion-level model[b]		
μQFR (≤0.80 vs >0.80)	1.46 (0.71-3.01)	0.304
TCFA	4.46 (2.33-8.56)	<0.001

[a]In the patient-level analysis, the primary endpoint occurred in 59 patients, comprising 20 patients with cardiac death and 39 patients with NCL-related events (10 patients with non-fatal myocardial infarctions and 36 patients with unplanned coronary revascularisations). The baseline variables that were considered clinically relevant (age, sex, coronary risk factors and clinical presentation) were entered in the patient-level model. [b]In the lesion-level analysis, 42 evaluable NCLs (11 NCLs with a non-fatal myocardial infarction and 39 NCLs with an unplanned coronary revascularisation) with angiography at the time of event and matched baseline OCT were determined in 39 patients. Cardiac deaths were not included in the lesion-level analysis. The other OCT characteristics with significant effects on clinical outcomes in the univariable analysis (MLA and non-culprit plaque rupture) that were identified within the same lesion were entered in the lesion-level model. μQFR: Murray fractal law-based quantitative flow ratio; CI: confidence interval; HR: hazard ratio; MLA: minimal lumen area; NCL: non-culprit lesion; OCT: optical coherence tomography; TCFA: thin-cap fibroatheroma

demonstrate a significant predictive value in either group. Detailed results of other covariates have been provided in **Supplementary Table 6**.

Discussion

This large-scale observational analysis integrated μQFR values with OCT-defined TCFA at the time of primary PCI to evaluate the long-term prognostic implications of NCLs in patients presenting with an AMI. Our findings revealed that an OCT-defined TCFA was more prevalent in NCLs with a μQFR ≤0.80; however, no independent association between these parameters was identified. The highest risk of adverse events was observed in patients and lesions with μQFR ≤0.80 combined with OCT-defined TCFA. Importantly, OCT-defined TCFA provided a significant incremental prognostic value, irrespective of μQFR values or the clinical presentation of AMI at admission. Conversely, the prognostic relevance of a μQFR ≤0.80 was relatively limited and primarily evident only when TCFA was also present. These insights have underscored the critical prognostic significance of OCT-identified NCL TCFA during the index procedure, demonstrating greater clinical relevance than μQFR for long-term clinical outcomes in an AMI population **(Central illustration)**.

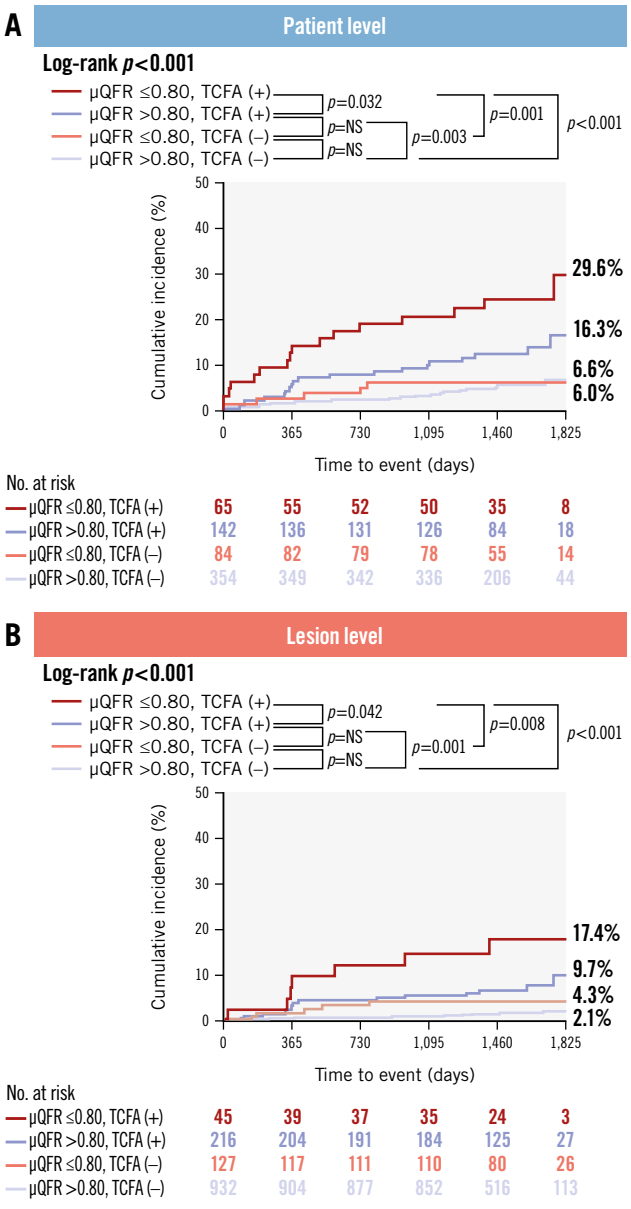

Figure 4. *Combined prognostic value of μQFR and OCT-defined TCFA in patient-level and lesion-level analyses. A significant difference in the risk of NCL-related clinical events was observed when categorising (A) patients and (B) lesions into four groups based on μQFR values and the presence or absence of TCFA. μQFR: Murray fractal law-based quantitative flow ratio; NS: non-significant; OCT: optical coherence tomography; TCFA: thin-cap fibroatheroma*

ASSESSMENT OF NCLS BASED ON μQFR AND OCT-DEFINED TCFA

Coronary physiology and plaque morphology are two dimensions for assessing NCLs, and a pathophysiological interplay exists between these factors[4,29]. Multiple investigations conducted on mixed populations comprising both stable coronary artery disease (CAD) and acute coronary syndrome patients have suggested an independent association between pressure wire-based haemodynamic significance and the presence of OCT-defined TCFA[30-32]. In contrast to these studies, our study recognised that OCT-defined TCFA was not an independent determinant of physiological severity as assessed by μQFR. The reason for this discrepancy may be that, although several studies using FFR[19] and three-dimensional (3D)-QFR[33] as references have demonstrated that the computation of μQFR from a single angiographic view has high feasibility and excellent diagnostic accuracy in identifying haemodynamically significant coronary stenosis, the existing evidence is still insufficient to support μQFR as a complete substitute for pressure wire-based FFR methods in accurately reflecting the true physiological status of plaques during the index procedure for AMI. This limitation might partly explain the lack of association observed in our study. In the present study, although the analysis of OCT imaging and offline μQFR calculations were performed retrospectively, both the OCT pullback and the angiograms used for μQFR were obtained at the time of the index procedure. This methodology allowed for a comprehensive assessment of NCLs in AMI patients undergoing primary or urgent PCI, providing greater convenience and minimising additional procedural risks, thus offering a distinct advantage over previous studies that primarily utilised FFR for similar evaluations. To summarise, our findings suggest that the impact of TCFA on clinical outcomes is independent of its interplay with coronary physiological characteristics, particularly in the context of AMI.

Table 4. Adjusted risk for μQFR ≤0.80 and OCT-defined TCFA in STEMI and non-STEMI patients.

	Adjusted HR (95% CI)	*p*-value
STEMI		
μQFR (≤0.80 vs >0.80)	1.75 (0.89-3.45)	0.104
TCFA	3.27 (1.67-6.41)	0.001
Non-STEMI		
μQFR (≤0.80 vs >0.80)	0.69 (0.21-2.27)	0.542
TCFA	3.26 (1.24-8.54)	0.016

Model adjustments are consistent with those applied in **Table 3**.
μQFR: Murray fractal law-based quantitative flow ratio; CI: confidence interval; HR: hazard ratio; OCT: optical coherence tomography; STEMI: ST-segment elevation myocardial infarction; TCFA: thin-cap fibroatheroma

RISK STRATIFICATION ACCORDING TO μQFR AND OCT-DEFINED TCFA

The evaluation of clinical outcomes based on μQFR assessment and OCT examination has not been comprehensively reported. In the present study, the risk of clinical events was highest in patients with acute μQFR ≤0.80 and OCT-defined TCFA (29.6%), followed by those with μQFR >0.80 and OCT-defined TCFA (16.3%); in both of these patient groups, the risk of clinical events was higher than in those without TCFA, where the predictive value of a μQFR ≤0.80 was insignificant. Similar trends were observed in the lesion-specific analysis. These findings align with the multivariate regression model, demonstrating an independent association between TCFA and clinical events, rather than μQFR values. Our study also demonstrated that TCFA

EuroIntervention Central Illustration

OCT-defined NCL TCFA demonstrates superior prognostic value compared to μQFR-determined functional significance

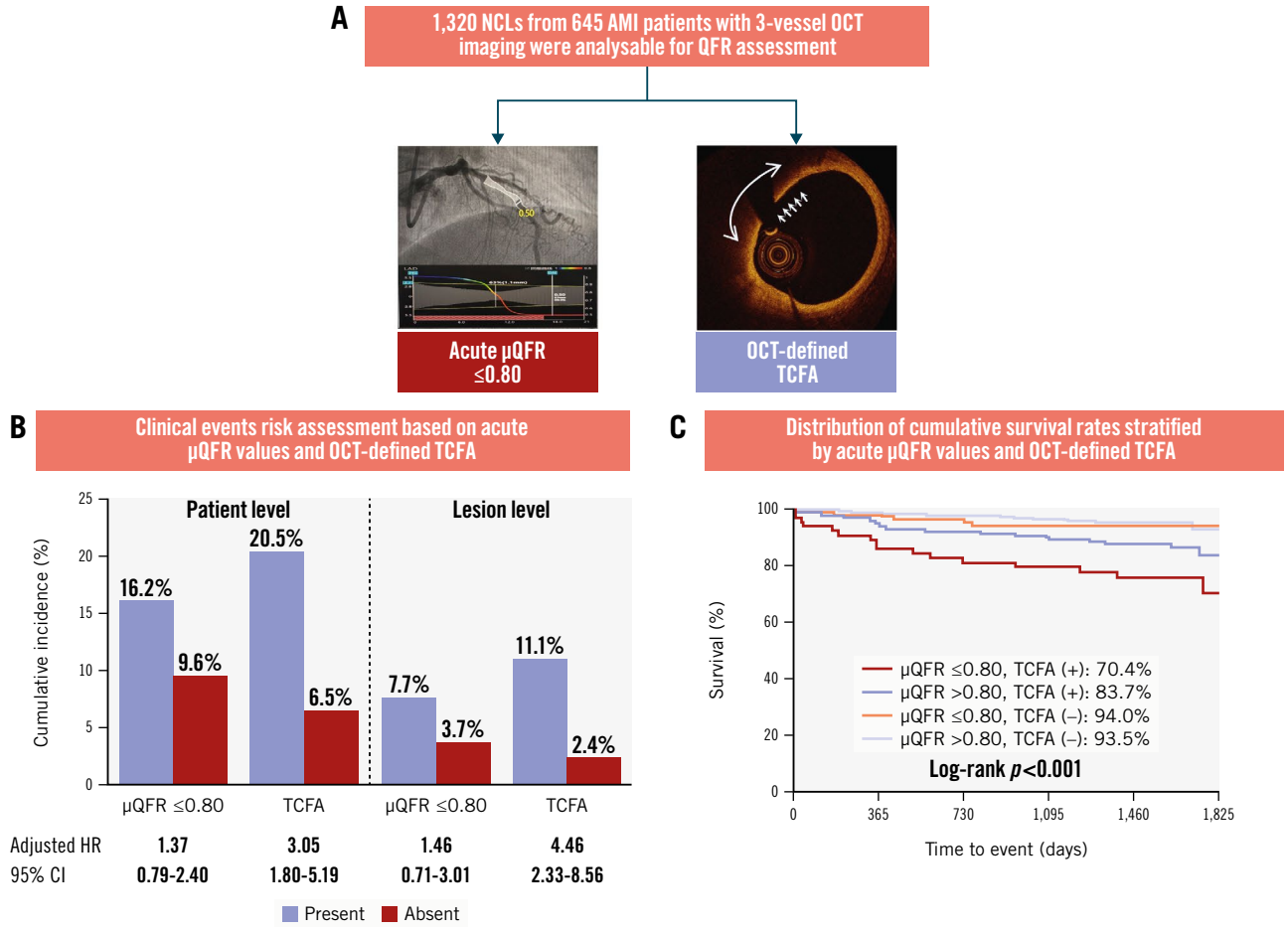

Xueming Xu *et al.* • *EuroIntervention* 2025;21:e217-e228 • DOI: 10.4244/EIJ-D-24-00720

A) Optical coherence tomography (OCT) examination and Murray fractal law-based quantitative flow ratio (μQFR) assessment were systematically conducted on a total of 1,320 non-culprit lesions (NCLs) from 645 patients with acute myocardial infarction (AMI), with a median follow-up period of 4.1 years (IQR 3.7-4.7). During the index procedure, OCT-defined thin-cap fibroatheroma (TCFA) demonstrated a dominant prognostic value for patient-level and lesion-specific adverse clinical events related to NCLs, whereas the μQFR-determined functional significance was insignificant. B) Clinical events risk assessment and (C) the cumulative survival rates. CI: confidence interval; HR: hazard ratio; IQR: interquartile range

provided significant prognostic information in both STEMI and NSTEMI patients, indicating that it is not influenced by the clinical environment, thus proving to be a more robust predictor compared to μQFR. Recently, Seike et al demonstrated that lesion-specific intravascular ultrasound (IVUS)-derived FFR ≤0.95 was an independent predictor of non-culprit clinical endpoints, alongside IVUS-defined plaque morphological characteristics[34]. Similarly, Safi et al found that a low but normal QFR (>0.80 to <0.97) provided additional prognostic information beyond plaque morphology for predicting clinical endpoints up to 5 years[35]. However, these findings do not conflict with our results. Our study aimed to demonstrate that OCT-defined TCFA offered significant prognostic value compared to μQFR-determined functional significance (defined as ≤0.80). In future research, we plan to investigate the optimal μQFR threshold for diagnosing lesion-specific clinical events and explore its clinical significance in comparison to OCT-defined TCFA. Furthermore, we found that in NCLs with μQFR >0.80, OCT-defined TCFA was significantly associated with a higher risk of clinical endpoints; contrastingly, the remaining μQFR-negative lesions without TCFA had a truly low risk of future adverse events. Numerous studies have previously reported the impact of high-risk plaque on clinical outcomes in non-ischaemic lesions. However, the present study differs substantially from previous reports in several ways. In the COMBINE OCT-FFR

(Optical Coherence Tomography Morphologic and Fractional Flow Reserve Assessment in Diabetes Mellitus Patients) study[21], OCT imaging was performed on 445 FFR-negative lesions in 390 patients with diabetes mellitus, 74.9% of whom had stable CAD, and follow-up was limited to 1.5 years. In the PECTUS-obs (Identification of Risk Factors for Acute Coronary Events by OCT After STEMI and NSTEMI in Patients With Residual Non-flow Limiting Lesions) study[36], 420 patients with MI underwent FFR assessment either during the index procedure or within 6 weeks in a staged approach, with subsequent OCT examination focused on specific lesions that were FFR-negative, and the follow-up was 2 years. Notably, a recent study reported that FFR values obtained during the acute phase of AMI decreased significantly over time, leading to false-negative results, while QFR remained relatively constant[16]. Therefore, the present study used μQFR instead of FFR to determine the functional significance of NCLs, and OCT imaging covered the non-IRAs to avoid missing high-risk NCLs. Based on these findings, the present study suggests that during the acute phase, OCT-defined TCFA may serve as a more critical prognostic predictor than acute μQFR assessment for long-term clinical outcomes related to NCLs in an AMI population. However, given the retrospective nature of this study, further prospective research is needed to confirm the superiority of OCT-defined plaque vulnerability, especially TCFA, over μQFR-derived coronary physiology in risk stratification and, potentially, in tailoring treatment.

Limitations

Several limitations should be considered when interpreting the results of this study. First, the single-centre and retrospective design of the present study may have introduced some selection bias. Additionally, as this study represents an initial exploratory analysis, it was not registered in a public registry, which may limit transparency and increase potential bias. Future studies will address this limitation by ensuring proper registration to enhance reproducibility and alignment with established research standards. Second, our findings pertain only to patients with AMI, and thus may not be generalisable to patients with stable CAD. However, similar results have been documented previously for the latter patient category[21,37]. Third, although OCT was performed on all three main coronary arteries, some distal small segments and branches were not examined. Moreover, a total of 468 NCLs in IRAs were excluded from the study due to issues with interpretation of acute μQFR IRA computation during the index procedure of AMI patients. Fourth, it was difficult to determine the origin of cardiac death without follow-up angiography. Consistent with previous studies[20,21], cardiac deaths that could not be clearly attributed to culprit lesions were classified as NCL-related in the patient-level analysis, which is probable given the treatment of the culprit lesion with contemporary PCI[3]. Fifth, given the presence of coronary microcirculatory dysfunction in patients with AMI, the reduced diagnostic performance of μQFR cannot be fully excluded[38]. Sixth, the findings of the present study are specific to μQFR and may not necessarily extend to other modalities such as QFR, OCT-based FFR, or pressure wire-based FFR and non-hyperaemic diastolic pressure ratios. Further research is required to determine whether similar results can be replicated using these alternative physiological assessment tools. Seventh, although we utilised the virtual stent technique embedded within the μQFR system to calculate each target NCL independently, thereby reducing the impact of tandem lesions, this influence cannot be completely ruled out. Further studies are needed to better understand the effect of tandem lesions on μQFR calculations, their potential prognostic implications, and their relationship with plaque phenotype. Finally, a small number of patients were evaluated at the 5-year follow-up. However, the Kaplan-Meier curves continued to diverge at both the patient and lesion levels, indicating a potentially higher HR for future clinical events if all patients completed the 5-year follow-up.

Conclusions

During the index procedure in an AMI population, OCT-identified NCL TCFA serves as a more dominant and independent prognostic indicator for long-term clinical outcomes than μQFR-determined physiological significance, emphasising the critical role of OCT as a powerful tool for identifying high-risk patients and its potential for tailoring treatment.

Authors' affiliations

1. State Key Laboratory of Frigid Zone Cardiovascular Diseases (SKLFZCD), Harbin, China; 2. Department of Cardiology, The Second Affiliated Hospital of Harbin Medical University, Harbin, China; 3. Key Laboratory of Myocardial Ischemia, Chinese Ministry of Education, Harbin, China; 4. Cardiovascular Research Foundation, New York, NY, USA

Acknowledgements

The authors thank all the participating patients for their contributions to the study.

Funding

This work was supported by the National Natural Science Foundation of China, grant no. 82322036 (to Dr Dai), 82072091 (to Dr Dai), 62135002 (to Dr Yu), 82202286 (to Dr Fang), and the Natural Science Foundation of Heilongjiang Province, grant no. YQ2023H014 (to Dr Fang).

Conflict of interest statement

The authors have no conflicts of interest to declare.

References

1. Park DW, Clare RM, Schulte PJ, Pieper KS, Shaw LK, Califf RM, Ohman EM, Van de Werf F, Hirji S, Harrington RA, Armstrong PW, Granger CB, Jeong MH, Patel MR. Extent, location, and clinical significance of non-infarct-related coronary artery disease among patients with ST-elevation myocardial infarction. *JAMA*. 2014;312:2019-27.
2. Tripathi B, Yeh RW, Bavishi CP, Sardar P, Atti V, Mukherjee D, Bashir R, Abbott JD, Giri J, Chatterjee S. Etiologies, trends, and predictors of readmission in ST-elevation myocardial infarction patients undergoing multivessel percutaneous coronary intervention. *Catheter Cardiovasc Interv*. 2019;94:905-14.
3. Scirica BM, Bergmark BA, Morrow DA, Antman EM, Bonaca MP, Murphy SA, Sabatine MS, Braunwald E, Wiviott SD. Nonculprit Lesion Myocardial Infarction Following Percutaneous Coronary Intervention in Patients With Acute Coronary Syndrome. *J Am Coll Cardiol*. 2020;75:1095-106.

4. Ahmadi A, Stone GW, Leipsic J, Serruys PW, Shaw L, Hecht H, Wong G, Nørgaard BL, O'Gara PT, Chandrashekhar Y, Narula J. Association of Coronary Stenosis and Plaque Morphology With Fractional Flow Reserve and Outcomes. *JAMA Cardiol.* 2016;1:350-7.

5. van der Hoeven NW, Janssens GN, de Waard GA, Everaars H, Broyd CJ, Beijnink CWH, van de Ven PM, Nijveldt R, Cook CM, Petraco R, Ten Cate T, von Birgelen C, Escaned J, Davies JE, van Leeuwen MAH, van Royen N. Temporal Changes in Coronary Hyperemic and Resting Hemodynamic Indices in Nonculprit Vessels of Patients With ST-Segment Elevation Myocardial Infarction. *JAMA Cardiol.* 2019;4:736-44.

6. Thim T, Götberg M, Fröbert O, Nijveldt R, van Royen N, Baptista SB, Koul S, Kellerth T, Bøtker HE, Terkelsen CJ, Christiansen EH, Jakobsen L, Kristensen SD, Maeng M. Nonculprit Stenosis Evaluation Using Instantaneous Wave-Free Ratio in Patients With ST-Segment Elevation Myocardial Infarction. *JACC Cardiovasc Interv.* 2017;10:2528-35.

7. Escaned J, Ryan N, Mejía-Rentería H, Cook CM, Dehbi HM, Alegria-Barrero E, Alghamdi A, Al-Lamee R, Altman J, Ambrosia A, Baptista SB, Bertilsson M, Bhindi R, Birgander M, Bojara W, Brugaletta S, Buller C, Calais F, Silva PC, Carlsson J, Christiansen EH, Danielewicz M, Di Mario C, Doh JH, Erglis A, Erlinge D, Gerber RT, Going O, Gudmundsdottir I, Härle T, Hauer D, Hellig F, Indolfi C, Jakobsen L, Janssens L, Jensen J, Jeremias A, Kåregren A, Karlsson AC, Kharbanda RK, Khashaba A, Kikuta Y, Krackhardt F, Koo BK, Koul S, Laine M, Lehman SJ, Lindroos P, Malik IS, Maeng M, Matsuo H, Meuwissen M, Nam CW, Niccoli G, Nijjer SS, Olsson H, Olsson SE, Omerovic E, Panayi G, Petraco R, Piek JJ, Ribichini F, Samady H, Samuels B, Sandhall L, Sapontis J, Sen S, Seto AH, Sezer M, Sharp ASP, Shin ES, Singh J, Takashima H, Talwar S, Tanaka N, Tang K, Van Belle E, van Royen N, Varenhorst C, Vinhas H, Vrints CJ, Walters D, Yokoi H, Fröbert O, Patel MR, Serruys P, Davies JE, Götberg M. Safety of the Deferral of Coronary Revascularization on the Basis of Instantaneous Wave-Free Ratio and Fractional Flow Reserve Measurements in Stable Coronary Artery Disease and Acute Coronary Syndromes. *JACC Cardiovasc Interv.* 2018;11:1437-49.

8. Hakeem A, Edupuganti MM, Almomani A, Pothineni NV, Payne J, Abualsuod AM, Bhatti S, Ahmed Z, Uretsky BF. Long-Term Prognosis of Deferred Acute Coronary Syndrome Lesions Based on Nonischemic Fractional Flow Reserve. *J Am Coll Cardiol.* 2016;68:1181-91.

9. Puymirat E, Cayla G, Simon T, Steg PG, Montalescot G, Durand-Zaleski I, le Bras A, Gallet R, Khalife K, Morelle JF, Motreff P, Lemesle G, Dillinger JG, Lhermusier T, Silvain J, Roule V, Labèque JN, Rangé G, Ducrocq G, Cottin Y, Blanchard D, Charles Nelson A, De Bruyne B, Chatellier G, Danchin N; FLOWER-MI Study Investigators. Multivessel PCI Guided by FFR or Angiography for Myocardial Infarction. *N Engl J Med.* 2021;385:297-308.

10. Lee JM, Kim HK, Park KH, Choo EH, Kim CJ, Lee SH, Kim MC, Hong YJ, Ahn SG, Doh JH, Lee SY, Park SD, Lee HJ, Kang MG, Koh JS, Cho YK, Nam CW, Koo BK, Lee BK, Yun KH, Hong D, Joh HS, Choi KH, Park TK, Yang JH, Song YB, Choi SH, Gwon HC, Hahn JY; FRAME-AMI Investigators. Fractional flow reserve versus angiography-guided strategy in acute myocardial infarction with multivessel disease: a randomized trial. *Eur Heart J.* 2023;44:473-84.

11. Böhm F, Mogensen B, Engstrøm T, Stankovic G, Srdanovic I, Lønborg J, Zwackman S, Hamid M, Kellerth T, Lauermann J, Kajander OA, Andersson J, Linder R, Angerås O, Renlund H, Êrglis A, Menon M, Schultz C, Laine M, Held C, Rück A, Östlund O, James S; FULL REVASC Trial Investigators. FFR-Guided Complete or Culprit-Only PCI in Patients with Myocardial Infarction. *N Engl J Med.* 2024;390:1481-92.

12. Tu S, Westra J, Yang J, von Birgelen C, Ferrara A, Pellicano M, Nef H, Tebaldi M, Murasato Y, Lansky A, Barbato E, van der Heijden LC, Reiber JHC, Holm NR, Wijns W; FAVOR Pilot Trial Study Group. Diagnostic Accuracy of Fast Computational Approaches to Derive Fractional Flow Reserve From Diagnostic Coronary Angiography: The International Multicenter FAVOR Pilot Study. *JACC Cardiovasc Interv.* 2016;9:2024-35.

13. Xu B, Tu S, Qiao S, Qu X, Chen Y, Yang J, Guo L, Sun Z, Li Z, Tian F, Fang W, Chen J, Li W, Guan C, Holm NR, Wijns W, Hu S. Diagnostic Accuracy of Angiography-Based Quantitative Flow Ratio Measurements for Online Assessment of Coronary Stenosis. *J Am Coll Cardiol.* 2017;70:3077-87.

14. Westra J, Andersen BK, Campo G, Matsuo H, Koltowski L, Eftekhari A, Liu T, Di Serafino L, Di Girolamo D, Escaned J, Nef H, Naber C, Barbierato M, Tu S, Neghabat O, Madsen M, Tebaldi M, Tanigaki T, Kochman J, Somi S, Esposito G, Mercone G, Mejia-Renteria H, Ronco F, Bøtker HE, Wijns W, Christiansen EH, Holm NR. Diagnostic Performance of In-Procedure Angiography-Derived Quantitative Flow Reserve Compared to Pressure-Derived Fractional Flow Reserve: The FAVOR II Europe-Japan Study. *J Am Heart Assoc.* 2018;7:e009603.

15. Xu B, Tu S, Song L, Jin Z, Yu B, Fu G, Zhou Y, Wang J, Chen Y, Pu J, Chen L, Qu X, Yang J, Liu X, Guo L, Shen C, Zhang Y, Zhang Q, Pan H, Fu X, Liu J, Zhao Y, Escaned J, Wang Y, Fearon WF, Dou K, Kirtane AJ, Wu Y, Serruys PW, Yang W, Wijns W, Guan C, Leon MB, Qiao S, Stone GW; FAVOR III China study group. Angiographic quantitative flow ratio-guided coronary intervention (FAVOR III China): a multicentre, randomised, sham-controlled trial. *Lancet.* 2021;398:2149-59.

16. Wang L, Travieso A, van der Hoeven N, van Leeuwen MAH, Janssens G, Mejía-Rentería H, Jerónimo A, Gonzalo N, Nijveldt R, van Royen N, Escaned J. Improved Nonculprit Stenosis Assessment in Patients With ST-Segment Elevation Myocardial Infarction Using Quantitative Flow Ratio. *JACC Cardiovasc Interv.* 2023;16:1828-30.

17. Erriquez A, Campo G, Guiducci V, Casella G, Menozzi M, Cerrato E, Sacchetta G, Moreno R, Arena M, Amat Santos I, Diez Gil JL, Scarsini R, Ruozzi M, Arioti M, Picchi A, Barbierato M, Moscarella E, Musto D'Amore S, Lanzilotti V, Cavazza C, Rezzaghi M, Cocco M, Marrone A, Verardi FM, Escaned J, Barbato E, Colaiori I, Pesenti N, Carrara G, Biscaglia S. QFR for the Revascularization of Nonculprit Vessels in MI Patients: Insights From the FIRE Trial. *JACC Cardiovasc Interv.* 2024;17:1425-36.

18. Lauri FM, Macaya F, Mejía-Rentería H, Goto S, Yeoh J, Nakayama M, Quirós A, Liontou C, Pareek N, Fernández-Ortíz A, Macaya C, MacCarthy P, Escaned J; Collaborators. Angiography-derived functional assessment of non-culprit coronary stenoses in primary percutaneous coronary intervention. *EuroIntervention.* 2020;15:e1594-601.

19. Tu S, Ding D, Chang Y, Li C, Wijns W, Xu B. Diagnostic accuracy of quantitative flow ratio for assessment of coronary stenosis significance from a single angiographic view: A novel method based on bifurcation fractal law. *Catheter Cardiovasc Interv.* 2021;97:1040-7.

20. Prati F, Romagnoli E, Gatto L, La Manna A, Burzotta F, Ozaki Y, Marco V, Boi A, Fineschi M, Fabbiocchi F, Taglieri N, Niccoli G, Trani C, Versaci F, Calligaris G, Ruscica G, Di Giorgio A, Vergallo R, Albertucci M, Biondi-Zoccai G, Tamburino C, Crea F, Alfonso F, Arbustini E. Relationship between coronary plaque morphology of the left anterior descending artery and 12 months clinical outcome: the CLIMA study. *Eur Heart J.* 2020;41:383-91.

21. Kedhi E, Berta B, Roleder T, Hermanides RS, Fabris E, IJsselmuiden AJJ, Kauer F, Alfonso F, von Birgelen C, Escaned J, Camaro C, Kennedy MW, Pereira B, Magro M, Nef H, Reith S, Al Nooryani A, Rivero F, Malinowski K, De Luca G, Garcia Garcia H, Granada JF, Wojakowski W. Thin-cap fibroatheroma predicts clinical events in diabetic patients with normal fractional flow reserve: the COMBINE OCT-FFR trial. *Eur Heart J.* 2021;42:4671-9.

22. Jiang S, Fang C, Xu X, Xing L, Sun S, Peng C, Yin Y, Lei F, Wang Y, Li L, Chen Y, Pei X, Jia R, Tang C, Li S, Li S, Yu H, Chen T, Tan J, Liu X, Hou J, Dai J, Yu B. Identification of High-Risk Coronary Lesions by 3-Vessel Optical Coherence Tomography. *J Am Coll Cardiol.* 2023;81:1217-30.

23. Guan S, Gan Q, Han W, Zhai X, Wang M, Chen Y, Zhang L, Li T, Chang X, Liu H, Hong W, Li Z, Tu S, Qu X. Feasibility of Quantitative Flow Ratio Virtual Stenting for Guidance of Serial Coronary Lesions Intervention. *J Am Heart Assoc.* 2022;11:e025663.

24. Lee SH, Hong D, Shin D, Kim HK, Park KH, Choo EH, Kim CJ, Kim MC, Hong YJ, Ahn SG, Doh JH, Lee SY, Park SD, Lee HJ, Kang MG, Koh JS, Cho YK, Nam CW, Joh HS, Choi KH, Park TK, Yang JH, Song YB, Choi SH, Jeong MH, Gwon HC, Hahn JY, Lee JM; FRAME-AMI Investigators. QFR Assessment and Prognosis After Nonculprit PCI in Patients With Acute Myocardial Infarction. *JACC Cardiovasc Interv.* 2023;16:2365-79.

25. Tearney GJ, Regar E, Akasaka T, Adriaenssens T, Barlis P, Bezerra HG, Bouma B, Bruining N, Cho JM, Chowdhary S, Costa MA, de Silva R, Dijkstra J, Di Mario C, Dudek D, Falk E, Feldman MD, Fitzgerald P, Garcia-Garcia HM, Gonzalo N, Granada JF, Guagliumi G, Holm NR, Honda Y, Ikeno F, Kawasaki M, Kochman J, Koltowski L, Kubo T, Kume T, Kyono H, Lam CC, Lamouche G, Lee DP, Leon MB, Maehara A,

Manfrini O, Mintz GS, Mizuno K, Morel MA, Nadkarni S, Okura H, Otake H, Pietrasik A, Prati F, Räber L, Radu MD, Rieber J, Riga M, Rollins A, Rosenberg M, Sirbu V, Serruys PW, Shimada K, Shinke T, Shite J, Siegel E, Sonoda S, Suter M, Takarada S, Tanaka A, Terashima M, Thim T, Uemura S, Ughi GJ, van Beusekom HM, van der Steen AF, van Es GA, van Soest G, Virmani R, Waxman S, Weissman NJ, Weisz G; International Working Group for Intravascular Optical Coherence Tomography (IWG-IVOCT). Consensus standards for acquisition, measurement, and reporting of intravascular optical coherence tomography studies: a report from the International Working Group for Intravascular Optical Coherence Tomography Standardization and Validation. *J Am Coll Cardiol.* 2012;59:1058-72.

26. Shimokado A, Matsuo Y, Kubo T, Nishiguchi T, Taruya A, Teraguchi I, Shiono Y, Orii M, Tanimoto T, Yamano T, Ino Y, Hozumi T, Tanaka A, Muragaki Y, Akasaka T. In vivo optical coherence tomography imaging and histopathology of healed coronary plaques. *Atherosclerosis.* 2018;275:35-42.

27. Araki M, Park SJ, Dauerman HL, Uemura S, Kim JS, Di Mario C, Johnson TW, Guagliumi G, Kastrati A, Joner M, Holm NR, Alfonso F, Wijns W, Adriaenssens T, Nef H, Rioufol G, Amabile N, Souteyrand G, Meneveau N, Gerbaud E, Opolski MP, Gonzalo N, Tearney GJ, Bouma B, Aguirre AD, Mintz GS, Stone GW, Bourantas CV, Räber L, Gili S, Mizuno K, Kimura S, Shinke T, Hong MK, Jang Y, Cho JM, Yan BP, Porto I, Niccoli G, Montone RA, Thondapu V, Papafaklis MI, Michalis LK, Reynolds H, Saw J, Libby P, Weisz G, Iannaccone M, Gori T, Toutouzas K, Yonetsu T, Minami Y, Takano M, Raffel OC, Kurihara O, Soeda T, Sugiyama T, Kim HO, Lee T, Higuma T, Nakajima A, Yamamoto E, Bryniarski KL, Di Vito L, Vergallo R, Fracassi F, Russo M, Seegers LM, McNulty I, Park S, Feldman M, Escaned J, Prati F, Arbustini E, Pinto FJ, Waksman R, Garcia-Garcia HM, Maehara A, Ali Z, Finn AV, Virmani R, Kini AS, Daemen J, Kume T, Hibi K, Tanaka A, Akasaka T, Kubo T, Yasuda S, Croce K, Granada JF, Lerman A, Prasad A, Regar E, Saito Y, Sankardas MA, Subban V, Weissman NJ, Chen Y, Yu B, Nicholls SJ, Barlis P, West NEJ, Arbab-Zadeh A, Ye JC, Dijkstra J, Lee H, Narula J, Crea F, Nakamura S, Kakuta T, Fujimoto J, Fuster V, Jang IK. Optical coherence tomography in coronary atherosclerosis assessment and intervention. *Nat Rev Cardiol.* 2022;19:684-703.

28. Cutlip DE, Windecker S, Mehran R, Boam A, Cohen DJ, van Es GA, Steg PG, Morel MA, Mauri L, Vranckx P, McFadden E, Lansky A, Hamon M, Krucoff MW, Serruys PW; Academic Research Consortium. Clinical end points in coronary stent trials: a case for standardized definitions. *Circulation.* 2007;115:2344-51.

29. Yang S, Koo BK, Narula J. Interactions Between Morphological Plaque Characteristics and Coronary Physiology: From Pathophysiological Basis to Clinical Implications. *JACC Cardiovasc Imaging.* 2022;15:1139-51.

30. Kanno Y, Sugiyama T, Hoshino M, Usui E, Hamaya R, Kanaji Y, Murai T, Lee T, Yonetsu T, Kakuta T. Optical coherence tomography-defined plaque vulnerability in relation to functional stenosis severity stratified by fractional flow reserve and quantitative flow ratio. *Catheter Cardiovasc Interv.* 2020;96:E238-47.

31. Usui E, Yonetsu T, Kanaji Y, Hoshino M, Yamaguchi M, Hada M, Fukuda T, Sumino Y, Ohya H, Hamaya R, Kanno Y, Yuki H, Murai T, Lee T, Hirao K, Kakuta T. Optical Coherence Tomography-Defined Plaque Vulnerability in Relation to Functional Stenosis Severity and Microvascular Dysfunction. *JACC Cardiovasc Interv.* 2018;11:2058-68.

32. Usui E, Yonetsu T, Murai T, Kanaji Y, Matsuda J, Hoshino M, Araki M, Niida T, Hada M, Ichijyo S, Hamaya R, Kanno Y, Lee T, Isobe M, Kakuta T. Prevalence of Thin-Cap Fibroatheroma in Relation to the Severity of Anatomical and Physiological Stenosis. *Circ J.* 2017;81:1816-23.

33. Cortés C, Liu L, Berdin SL, Fernández-Corredoira PM, Zhang R, Schäfer U, López M, Diarte JA, Tu S, Gutiérrez-Chico JL. Agreement between Murray law-based quantitative flow ratio (μQFR) and three-dimensional quantitative flow ratio (3D-QFR) in non-selected angiographic stenosis: A multicenter study. *Cardiol J.* 2022;29:388-95.

34. Seike F, Mintz GS, Matsumura M, Ali ZA, Liu M, Jeremias A, Ben-Yehuda O, De Bruyne B, Serruys PW, Yasuda K, Stone GW, Maehara A. Impact of Intravascular Ultrasound-Derived Lesion-Specific Virtual Fractional Flow Reserve Predicts 3-Year Outcomes of Untreated Nonculprit Lesions: The PROSPECT Study. *Circ Cardiovasc Interv.* 2022;15:851-60.

35. Safi H, Bourantas CV, Ramasamy A, Zanchin T, Bär S, Tufaro V, Jin C, Torii R, Karagiannis A, Reiber JHC, Mathur A, Onuma Y, Windecker S, Lansky A, Maehara A, Serruys PW, Stone P, Baumbach A, Stone GW, Räber L. Predictive value of the QFR in detecting vulnerable plaques in non-flow limiting lesions: a combined analysis of the PROSPECT and IBIS-4 study. *Int J Cardiovasc Imaging.* 2020;36:993-1002.

36. Mol JQ, Volleberg RHJA, Belkacemi A, Hermanides RS, Meuwissen M, Protopopov AV, Laanmets P, Krestyaninov OV, Dennert R, Oemrawsingh RM, van Kuijk JP, Arkenbout K, van der Heijden DJ, Rasoul S, Lipsic E, Rodwell L, Camaro C, Damman P, Roleder T, Kedhi E, van Leeuwen MAH, van Geuns RM, van Royen N. Fractional Flow Reserve-Negative High-Risk Plaques and Clinical Outcomes After Myocardial Infarction. *JAMA Cardiol.* 2023;8:1013-21.

37. Lee JM, Choi KH, Koo BK, Park J, Kim J, Hwang D, Rhee TM, Kim HY, Jung HW, Kim KJ, Yoshiaki K, Shin ES, Doh JH, Chang HJ, Cho YK, Yoon HJ, Nam CW, Hur SH, Wang J, Chen S, Kuramitsu S, Tanaka N, Matsuo H, Akasaka T. Prognostic Implications of Plaque Characteristics and Stenosis Severity in Patients With Coronary Artery Disease. *J Am Coll Cardiol.* 2019;73:2413-24.

38. Mejía-Rentería H, Lee JM, Lauri F, van der Hoeven NW, de Waard GA, Macaya F, Pérez-Vizcayno MJ, Gonzalo N, Jiménez-Quevedo P, Nombela-Franco L, Salinas P, Núñez-Gil I, Del Trigo M, Goto S, Lee HJ, Liontou C, Fernández-Ortiz A, Macaya C, van Royen N, Koo BK, Escaned J. Influence of Microcirculatory Dysfunction on Angiography-Based Functional Assessment of Coronary Stenoses. *JACC Cardiovasc Interv.* 2018;11:741-53.

Supplementary data

Supplementary Appendix 1. Supplementary methods.

Supplementary Table 1. Independent predictors of per-lesion μQFR ≤0.80.

Supplementary Table 2. Diagnosis for multicollinearity.

Supplementary Table 3. Patients with adverse cardiac events during follow-up.

Supplementary Table 4. Independent predictors of NCL-related clinical events at the patient level.

Supplementary Table 5. Independent predictors of NCL-related clinical events at the lesion level.

Supplementary Table 6. Adjusted risk for μQFR ≤0.80 and OCT-defined TCFA in STEMI and NSTEMI patients.

Supplementary Figure 1. Prognostic implications of OCT-defined TCFA in patients and lesions, categorised by μQFR.

Supplementary Figure 2. Prognostic implications of μQFR values in patients and lesions, stratified by TCFA.

The supplementary data are published online at: https://eurointervention.pcronline.com/doi/10.4244/EIJ-D-24-00720

Supplementary data

Supplementary Appendix 1. Supplementary methods.

1. Diagnostic criteria for AMI

The diagnosis of acute myocardial infarction (AMI) includes two types: ST-segment elevation myocardial infarction (STEMI) and non-STEMI. STEMI is defined as persistent chest pain lasting at least 30 minutes, presentation to hospital within 12 hours of symptom onset, suggestive 12-lead ECG changes (ST-segment elevation >0.1 mV in ≥2 contiguous leads or documented newly developed left bundle-branch block), and elevation of cardiac biomarkers (creatine kinase-MB or troponin T/I). Non-STEMI is characterized by the presence of ischemic symptoms and elevated cardiac biomarkers, but without ST-segment elevation on the electrocardiogram.

2. Identification of culprit lesion at baseline

To identify the culprit lesion, abnormal manifestations of coronary angiography and electrocardiogram were considered. If necessary, an echocardiography or left ventricular angiogram was also performed to assess the culprit lesion. In patients with multiple stenoses, the lesion with the most severe stenosis or evidence of acute thrombus on OCT (if available) was deemed to be the culprit.

3. Detailed definitions of traditional coronary risk factors

Risk factors	Definition
Smoking status	1) Current smoker: active smoking ≤1 month 2) Former smoker: smoking cessation of >1 month 3) Non-smoker: no smoking at any time.
Hypertension	Patients with any one of the following: 1) Documented history of hypertension 2) Systolic blood pressure is 140 mmHg or greater 3) Diastolic blood pressure is 90 mmHg or greater 4) Active treatment with antihypertensive drugs.
Diabetes mellitus	Patients with at least one of the following: 1) Documented history of diabetes mellitus 2) Use of hypoglycemia agents

	3) Fasting glucose of ≥126 mg/dL 4) 2-hour plasma glucose level of ≥200 mg/dL in the oral glucose tolerance test 5) Classic symptom with casual plasma glucose level of ≥200 mg/dL 6) Hemoglobin A1c of ≥6.5%.
Dyslipidemia	Patients with any one of the following: 1) Documented history of hyperlipidemia 2) Treatment with a lipid lowering agent 3) Newly diagnosed with hyper lipidemia: • total cholesterol level of ≥220 mg/dL • triglycerides of ≥150 mg/ dL • low-density lipoprotein cholesterol of ≥140 mg/dL • high-density lipoprotein cholesterol of ≤40 mg/dL.
Chronic kidney disease	Estimated glomerular filtration rate (eGFR) <60 mL/min per 1.73m^2.

4. OCT analyses, and inter- and intra- observer agreement[25,26]

Expert readers at an independent core laboratory analyzed OCT images without knowledge of patient outcomes using an offline review workstation (Abbott Vascular) according to previously established criteria and consensus. NCLs were classified as either lipidic plaques (identified by a low signal region with diffuse borders) or fibrous plaques (characterized by a homogeneous and signal-rich region). The lumen area was automatically measured in every frame throughout the lesion and manually corrected if necessary, and the minimal lumen area (MLA) was determined. For each lipid plaque, the lipid arc was measured at 1 mm intervals throughout the entire lesion. The fibrous cap thickness (FCT) was measured three times at its thinnest point, and the average value was calculated. The length of the lipid core was recorded on the longitudinal OCT view. Non-culprit plaque rupture was identified by the presence of a fibrous cap discontinuity with a cavity formed inside the non-culprit plaques. Thrombus was defined as an irregular mass floating in or protruding into the lumen with a dimension of at least 250 μm. Calcification was defined as well-delineated, low backscattering heterogeneous regions. There was a possibility that the signal-poor regions behind the large calcium corresponded to lipid accumulation. However, OCT imaging cannot provide reliable analysis of tissue behind large calcium. In this situation, the calcium arc was measured

separately and did not calculate into the measurement of lipid arc. Macrophage accumulation was defined as signal-rich, distinct or confluent punctuate regions with heterogeneous backward shadowing. Microchannels were presented as signal-poor voids that are sharply delineated with a diameter of 50-300 μm visible in at least three consecutive cross-sections. Cholesterol crystals were identified by thin, linear and signal-rich regions within the plaque. Layered tissue was identified by one or more heterogeneous signal-rich layers of different optical signal density located close to the luminal surface with clear demarcation from the underlying plaque.

OCT imaging was analyzed by two blinded expert readers and a consensus reading was obtained from a third independent investigator when there was discordance between the two readers. Eighty patients were randomly selected to evaluate inter- and intra- observer agreement, as assessed by two independent investigators and by the same investigator at two separate time points with at least a two-week interval, respectively. The inter-observer agreement for TCFA, non-culprit plaque rupture, macrophage accumulation, and layered tissue was 0.86, 0.88, 0.77, and 0.81, respectively. The intra-observer agreement for TCFA, non-culprit plaque rupture, macrophage accumulation, and layered tissue was 0.92, 0.89, 0.82, 0.86, respectively.

5. Methodology of μQFR assessment

The study employed a new generation of AI-powered Murray law-based QFR (μQFR) for offline analysis, which enables automatic contour delineation and accurate FFR calculation from a single angiographic view. μQFR assessment was conducted retrospectively for all intermediate NCLs (30%-90% by visual estimation) in non-infarcted-related arteries by independent expert technicians who were blinded to OCT data and clinical outcomes using AngioPlus Core 2.0 (Pulse Medical Imaging Technology, Shanghai, China). The computation process comprises several key steps. First, a single angiographic projection with optimal visualization (minimal foreshortening and vessel overlap) containing the target NCL was chosen. Second, AI-powered algorithms were used to automatically generate the centerline of the vessel and calculate hyperemic flow velocity. This was achieved by dividing the length of the centerline by the contrast dye filling time. Third, a key frame with a sharp luminal contour on a major epicardial coronary artery containing the target NCL was then selected for subsequent analysis. Fourth, the luminal contours of the scanned vessels and major side branches were automatically delineated and manually corrected as necessary. Furthermore, the reference diameter function was reconstructed in accordance with the Murray fractal law. Finally, pressure drop was calculated using fluid dynamic equations with hyperemic flow velocity, providing

μQFR for the target NCL. A lesion was considered flow-limiting if the μQFR was ≤0.80.

6. Definitions of adverse cardiac events[28]

Adverse cardiac events included cardiac death, non-fatal myocardial infarction, and unplanned coronary revascularization, which were defined according to the Academic Research Consortium guideline. Cardiac death was defined as death from myocardial infarction, cardiac perforation or pericardial tamponade, arrhythmia or conduction abnormalities, procedural complications, or any death in which a cardiac cause could not be excluded. Non-fatal myocardial infarction was diagnosed by the detection of raise and fall of cardiac biomarkers (preferably troponin) above the 99th percentile of the upper reference limit, together with evidence of myocardial ischemia with at least one of the following criteria: ischemic symptoms; ECG changes indicative of new ischemia (new ST-T changes or new left bundle branch block); development of pathological Q waves in the ECG; and imaging evidence of new loss of viable myocardium or new regional wall motion abnormalities. Unplanned coronary revascularization was defined as any clinically driven (i.e., unstable angina or progressive angina) repeat percutaneous coronary intervention or surgical coronary artery bypass grafting, which initially was not planned after the index angiography and enrollment in the study.

Supplementary Table 1. Independent predictors of per-lesion μQFR ≤0.80.

	Univariate Analysis		Multivariable Analysis	
	Odds ratio (95% CI)	***P* Value**	**Odds ratio (95% CI)**	***P* Value**
OCT characteristics				
Lesions' location (LAD vs. LCX/RCA)	2.59 (1.87-3.58)	<0.001	2.23 (1.51-3.27)	<0.001
Distance from coronary ostium to MLA site, mm	1,00 (0.99-1.00)	0.357	-	-
Lipid core length, mm	1.04 (1.03-1.06)	<0.001	1.04 (1.02-1.05)	<0.001
TCFA	1.53 (1.06-2.22)	0.025	0.79 (0.51-1.21)	0.283
MLA, mm^2	0.38 (0.31-0.46)	<0.001	0.41 (0.34-0.51)	<0.001
Other qualitative characteristics				
Non-culprit plaque rupture	1.41 (0.81-2.44)	0.222	-	-
Thrombus	1.18 (0.52-2.67)	0.699	-	-
Calcification	1.24 (0.90-1.70)	0.197	-	-
Macrophage	2.09 (1.00-4.36)	0.051	-	-
Microchannel	0.88 (0.64-1.22)	0.448	-	-
Cholesterol crystals	1.73 (1.22-2.46)	0.002	0.83 (0.55-1.26)	0.388
Layered tissue	1.96 (1.41-2.73)	<0.001	0.93 (0.62-1.39)	0.719

CI, confidence interval; LAD, left anterior descending artery; LCX, left circumflex artery; MLA, minimum lumen area; OCT, optical coherence tomography; RCA, right coronary artery; TCFA, thin-cap fibroatheroma.

Supplementary Table 2. Diagnosis for multicollinearity.

Variable	Variance Inflation Factor	β	95% CI	*P* value
Lesions' location (LAD vs. LCX/RCA)	1.085	-0.173	(-0.052, -0.027)	<0.001
Lipid core length, mm	1.105	-0.211	(-0.003, -0.002)	<0.001
TCFA	1.067	-0.044	(-0.025, -0.003)	0.118
MLA, mm^2	1.099	0.322	(0.016, 0.022)	<0.001
Cholesterol crystals	1.055	-0.019	(-0.018, 0.009)	0.503
Layered tissue	1.118	-0.042	(-0.021, -0.003)	0.145

Abbreviations as in Supplementary Table 1.

Supplementary Table 3. Patients with adverse cardiac events during follow-up.

	All events	Culprit lesion-related events	Nonculprit lesion-related events	Indeterminate Events	The primary endpoint*
Adverse events, n	76	22	39	20	59
Cardiac death, n	20	0	0	20	20
Nonfatal myocardial infarction, n	15	5	10	0	10
Unplanned coronary revascularization, n	53	22	36	0	36

Values shown are n.

*The primary endpoint was the composite of cardiac death, non-culprit lesion-related nonfatal myocardial infarction and unplanned coronary revascularization.

Supplementary Table 4. Independent predictors of NCL-related clinical events at the patient level.

	Unadjusted HR (95% CI)	*P* Value	Adjusted HR (95% CI)	*P* Value
μQFR (≤0.80 vs >0.80)	**1.92 (1.13-3.28)**	**0.016**	**1.37 (0.79-2.40)**	**0.266**
OCT-defined plaque characteristics				
TCFA	**3.28 (1.95-5.51)**	**<0.001**	**3.05 (1.80-5.19)**	**<0.001**
MLA <3.5mm^2	2.68 (1.22-5.90)	0.014	2.21 (0.97-5.04)	0.059
Clinical baseline characteristics				
Age, years	1.01 (0.98-1.03)	0.525	1.00 (0.97-1.02)	0.683
Female	1.14 (0.65-2.01)	0.642	1.00 (0.55-1.82)	0.993
Current smoking	1.25 (0.75-2.09)	0.390	1.48 (0.86-2.57)	0.161
Hypertension	1.99 (1.18-3.36)	0.010	1.93 (1.13-3.30)	0.015
Dyslipidemia	0.97 (0.58-1.62)	0.895	0.94 (0.56-1.60)	0.830
Diabetes mellitus	1.26 (0.72-2.22)	0.419	1.06 (0.59-1.91)	0.849
CKD, eGFR <60 mL/min/1.73 m^2	2.35 (1.22-4.53)	0.011	2.25 (1.09-4.62)	0.028
ST-segment elevated myocardial infarction	0.78 (0.45-1.32)	0.351	0.81 (0.47-1.41)	0.456

In patient-level analysis, the primary endpoint occurred in 59 patients, comprising 20 patients with cardiac death and 39 patients with NCL-related events (10 patients with non-fatal myocardial infarctions and 36 patients with unplanned coronary revascularizations). The baseline variables that were considered clinically relevant (age, sex, coronary risk factors and clinical presentation) were entered in patient-level model. CI, confidence interval; CKD, chronic kidney disease; eGFR, estimated glomerular filtration rate; HR, hazard ratio; MLA, minimum lumen area; OCT, optical coherence tomography; μQFR: Murray fractal law-based quantitative flow ratio; TCFA, thin-cap fibroatheroma.

Supplementary Table 5. Independent predictors of NCL-related clinical events at the lesion level.

	Unadjusted HR (95% CI)	*P* Value	Adjusted HR (95% CI)	*P* Value
μQFR (≤0.80 vs >0.80)	**2.77 (1.42-5.41)**	**0.003**	**1.46 (0.71-3.01)**	**0.304**
OCT-defined plaque characteristics				
TCFA	**4.65 (2.54-8.52)**	**<0.001**	**4.46 (2.33-8.56)**	**<0.001**
MLA, mm^2	0.64 (0.50-0.82)	<0.001	0.68 (0.53-0.88)	0.003
Non-culprit plaque rupture	2.42 (1.08-5.46)	0.033	1.02 (0.43-2.43)	0.963
Thrombus	1.30 (0.32-5.40)	0.714	-	--
Calcification	1.04 (0.57-1.91)	0.903	-	
Macrophage	3.96 (0.55-28.81)	0.174	-	-
Microchannel	1.01 (0.55-1.86)	0.974	-	-
Cholesterol crystals	1.86 (0.99-3.50)	0.054	-	-
Layered tissue	1.30 (0.71-2.39)	0.400		-

In lesion-level analysis, 42 evaluable NCLs (11 NCLs with a non-fatal myocardial infarction and 39 NCLs with an unplanned coronary revascularization) with angiography at events and matched baseline OCT were determined in 39 patients. Cardiac deaths were not included in lesion-level analysis. The other OCT characteristics with significant effects on clinical outcomes in the univariable analysis (MLA and non-culprit plaque rupture) assessed within the same lesion were entered in lesion-level model. Abbreviations as in Supplementary Table 4

Supplementary Table 6. Adjusted risk for μQFR ≤0.80 and OCT-defined TCFA in STEMI and NSTEMI patients.

	STEMI		Non-STEMI	
	Adjusted HR (95% CI)	***P* Value**	**Adjusted HR (95% CI)**	***P* Value**
μQFR (≤0.80 vs >0.80)	**1.75 (0.89-3.45)**	**0.104**	**0.69 (0.21-2.27)**	**0.542**
OCT-defined plaque characteristics				
TCFA	**3.27 (1.67-6.41)**	**0.001**	**3.26 (1.24-8.54)**	**0.016**
MLA <3.5mm^2	2.77 (0.81-9.49)	0.106	2.07 (0.66-6.54)	0.214
Clinical baseline characteristics				
Age, years	1.01 (0.89-3.45)	0.496	0.96 (0.91-1.01)	0.080
Female	1.24 (0.60-2.57)	0.568	0.80 (0.28-2.34)	0.687
Current smoking	1.67 (0.82-3.37)	0.156	1.21 (0.49-3.00)	0.675
Hypertension	1.94 (0.98-3.83)	0.058	1.50 (0.62-3.63)	0.369
Dyslipidemia	1.12 (0.58-2.18)	0.731	0.70 (0.29-1.71)	0.434
Diabetes mellitus	0.82 (0.37-1.85)	0.639	1.25 (0.48-3.26)	0.646
CKD, eGFR <60 mL/min/1.73 m^2	2.52 (1.03-6.18)	0.043	2.84 (0.77-10.50)	0.117

CI, confidence interval; HR, hazard ratio; μQFR: Murray fractal law-based quantitative flow ratio; STEMI, ST-segment elevated myocardial infarction; TCFA, thin-cap fibroatheroma.

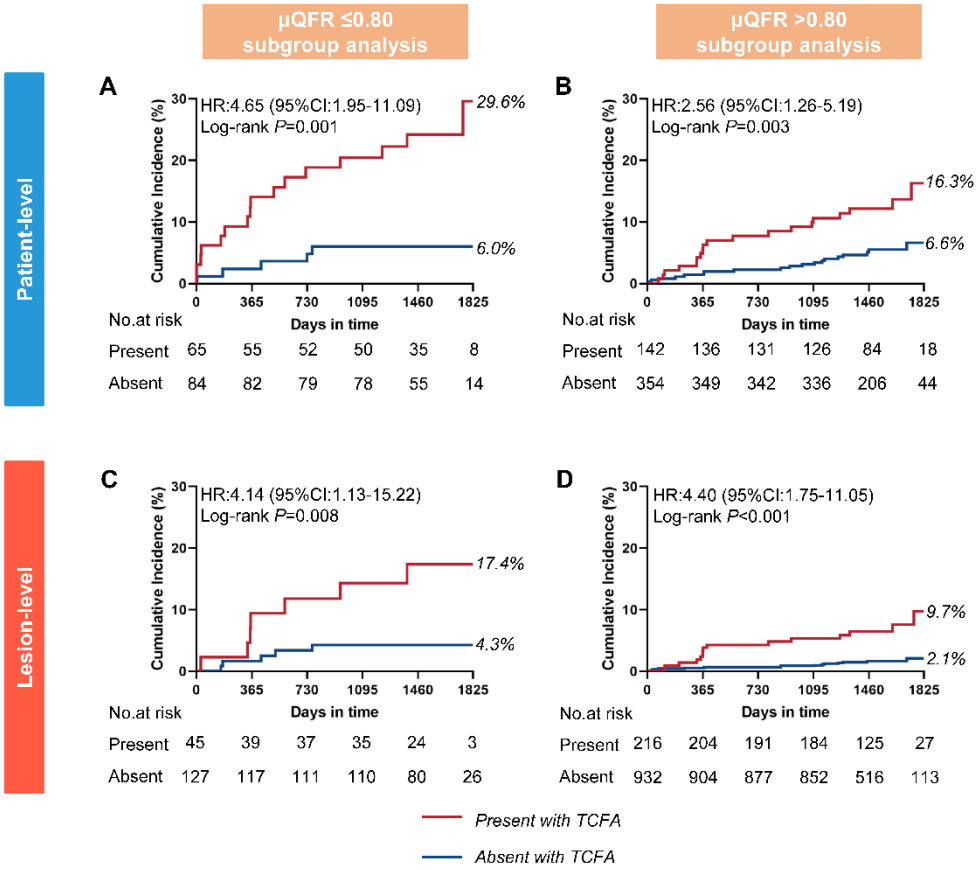

Supplementary Figure 1. Prognostic implications of OCT-defined TCFA in patients and lesions, categorised by μQFR.

A to B. The presence of OCT-defined TCFA is associated with a higher risk of the primary endpoint in patients with one or more NCLs with μQFR ≤0.80, as well as in those without NCLs with μQFR ≤0.80, respectively. **C to D** demonstrate that OCT-defined TCFAs are also associated with the cumulative incidence of lesion-specific event rates in NCLs with μQFR ≤0.80 and μQFR >0.80, respectively. CI, confidence interval; HR, hazard ratio; μQFR: Murray fractal law-based quantitative flow ratio; TCFA, thin-cap fibroatheroma.

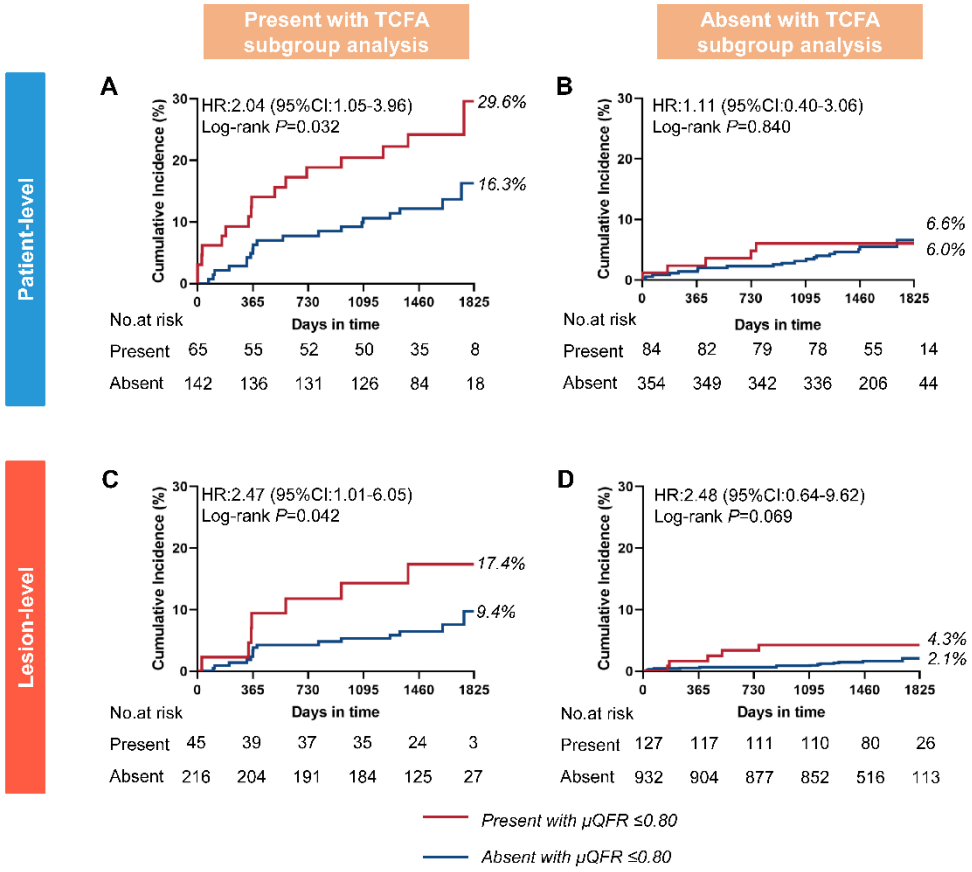

Supplementary Figure 2. Prognostic implications of μQFR values in patients and lesions, stratified by TCFA.

A. The presence of NCLs with μQFR ≤0.80 provides limit prognostic value for NCLs-related clinical events in patients with OCT-defined TCFA. **B.** The risk of NCLs-related clinical events was similar regardless of μQFR values in the subgroup without TCFA. **C and D.** The trends in lesion-level analysis were consistent with patient-level. Abbreviations as in Supplementary Figure 1.